# Three-Mode Optoacoustic Parametric Amplifier: A Tool for Macroscopic Quantum Experiments

Chunnong Zhao, Li Ju, Haixing Miao, Slawomir Gras, Yaohui Fan, and David G. Blair
*School of Physics, University of Western Australia, WA 6009, Australia*
(Received 21 September 2008; revised manuscript received 11 May 2009; published 17 June 2009)

We introduce the three-mode optoacoustic parametric amplifier (OAPA), a close analog of the optical parametric amplifier, for macroscopic quantum mechanics experiments. The radiation pressure reaction of light on the reflective surface of an acoustic resonator provides a nonlinearity similar to the Kerr effect in the optical parametric amplifier. The OAPA can be tuned to operate in a positive gain regime where acoustic signals are amplified or in a negative gain regime where acoustic modes are cooled. Compared with conventional optoacoustic devices, (i) the OAPA incorporates two transverse cavity modes such that the carrier and sideband fields simultaneously resonate, and (ii) it is less susceptible to the laser phase and amplitude noise. These two features significantly ease the experimental requirements for cooling of acoustic modes to their quantum-ground state and creating entangled pairs of phonons and photons.

DOI: 10.1103/PhysRevLett.102.243902 PACS numbers: 42.79.Jq, 42.50.Dv

*Introduction.*—Macroscopic devices based on three frequency interactions of electromagnetic waves have provided powerful tools across a range of disciplines from radio astronomy to quantum optics. In the 1960s, the nonlinear properties of varactor diodes were used to create extremely low noise nondegenerate parametric amplifiers for microwaves [1]. Besides, the Kerr effect in nonlinear optical crystals has been used to create optical parametric amplifiers (OPAs) and oscillators with a broad range of applications.

Recently, by coupling the acoustic mode of a resonator to one transverse cavity mode, various tabletop experiments [2–9] demonstrated that the thermal occupation number of the acoustic mode can be significantly reduced; i.e., this is called self-cooling in the literature. These experiments can eventually reach the quantum-ground state of a macroscopic resonator if the appropriate parameter regime is achieved [10–12]. The same scheme is also proposed to create stationary optoacoustic entanglement [13,14]. Different from those setups, here we consider a three-mode optoacoustic parametric amplifier (OAPA), in which two orthogonal transverse cavity modes interact with one acoustic mode. The device uses the intrinsic nonlinearity provided by the radiation pressure reaction of light on a reflective acoustic resonator to create a three-mode interacting system closely analogous to the OPA except that one channel is acoustic. The OAPA utilizes a resonant interaction among three high $Q$ factor resonators: two optical and one acoustic. Its classical mechanism was first introduced and analyzed by Braginsky *et al.* [15] in the context of long optical cavities for gravitational-wave detectors. The analysis was further elaborated in Refs. [16–19] to simulate the actual situation in typical advanced gravitational-wave detectors. More recently, we demonstrated a three-mode interaction experimentally in an 80 m optical cavity [20].

The three-mode parametric interaction can be considered as a scattering process between a high intensity optical carrier $\omega_0$ and a pair of acoustic and optical modes. The surface of an acoustic resonator of frequency $\omega_m$ serves as one end mirror of an optical cavity. The mirror scatters the carrier (usually the $\mathrm{TEM}_{00}$ mode) into upper and lower sidebands at frequencies of $\omega_0 + \omega_m$ and $\omega_0 - \omega_m$, respectively. If the *lower* sideband frequency is equal to a cavity transverse mode (e.g., the $\mathrm{TEM}_{01}$ mode) and thereby resonant inside the cavity, the scattering amplitude is resonantly enhanced, causing an amplification of the acoustic mode. Alternatively, if the *upper* sideband frequency is tuned to a cavity transverse mode frequency, the resonant scattering corresponds to the absorption of acoustic energy, thereby reducing the acoustic mode occupation number. Since both the carrier and the sideband optical fields are resonant inside the cavity, it significantly enhances the optoacoustic coupling, allows ground-state cooling of the acoustic mode, and creates optoacoustic entanglement with moderate input optical power.

Efficient three-mode parametric interaction requires that (i) the optical cavity must support eigenmodes that have a frequency difference (i.e., mode gap) approximately equal to the acoustic frequency and (ii) the optical and acoustic modes must have a suitable spatial overlap. In this Letter, we show that both conditions can be achieved in a benchtop centimeter-scale device with carefully designed optical and acoustic schemes. It can be potentially applied to very sensitive signal transduction and explorations of macroscopic quantum mechanics. We will show the experimental feasibility of realizing ground-state cooling of acoustic modes and creating stationary entanglement among phonons and photons with such devices.

*Quantitative description.*—As we have shown in Ref. [21], the OAPA can be described by the following Hamiltonian:

 

$$\hat{\mathcal{H}} = \tfrac{1}{2}\hbar\omega_m(\hat{q}_m^2 + \hat{p}_m^2) + \hbar\omega_0\hat{a}^\dagger\hat{a} + \hbar\omega_1\hat{b}^\dagger\hat{b} + \hbar G_0\hat{q}_m(\hat{a}^\dagger\hat{b} + \hat{b}^\dagger\hat{a}) + \hat{\mathcal{H}}_{\text{ext}}. \quad (1)$$

Here $\hat{q}_m$ and $\hat{p}_m$ are the dimensionless generalized position and momentum, respectively, of the acoustic mode oscillating at frequency $\omega_m$; $\hat{a}$ and $\hat{b}$ are the annihilation operators for the two cavity transverse modes, respectively, e.g., the $\text{TEM}_{00}$ and $\text{TEM}_{01}$ mode as being considered here; the coupling constant $G_0 \equiv \sqrt{\Lambda\hbar\omega_0\omega_1/(m\omega_m L^2)}$, with $\Lambda$ quantifying the overlap between the electromagnetic field pattern and the acoustic displacement pattern and $L$ denoting the length of the cavity; $\hat{\mathcal{H}}_{\text{ext}}$ describes the coupling between cavity modes and external continuum fields.

From the above Hamiltonian, we derived the detailed dynamic of the system via a standard Langevin equation approach [21]. The quantitative effectiveness of the parametric interaction is characterized by a dimensionless quantity—the parametric gain $\mathcal{R}$, first introduced in Ref. [15]. It depends on the product of three quality factors: those of the cavity modes $Q_0$ and $Q_1$ and of the acoustic mode $Q_m$. For a single interacting set of modes, $\mathcal{R}$ can be written as

$$\mathcal{R} = \frac{8I_{\text{in}}Q_0Q_1Q_m}{m\omega_0\omega_m^2L^2}\frac{\Lambda}{1 + (\Delta\omega/\gamma_1)^2}. \quad (2)$$

Here $I_{\text{in}}$ is the input laser power; $\Delta\omega \equiv |\omega_0 - \omega_1| - \omega_m$ is the frequency detuning, which is equal to zero in the resonant tuned case; $\gamma_1 \equiv \omega_1/(2Q_1)$ is the half linewidth (or damping rate) of the cavity transverse mode.

The optoacoustic coupling influences the dynamics of the acoustic mode. In particular, the damping rate $\gamma_m \equiv \omega_m/(2Q_m)$ of the acoustic mode is modified into an effective one $\gamma_m'$, which can be written as

$$\gamma_m' \approx (1 - \mathcal{R})\gamma_m. \quad (3)$$

For positive $\mathcal{R} < 1$, the amplitude of the acoustic mode is amplified by a factor $1/(1 - \mathcal{R})$. If $\mathcal{R} > 1$, the system becomes unstable, for which the acoustic mode amplitude increases exponentially with time until nonlinear losses lead to saturation. For negative values of $\mathcal{R}$, the cavity modes extract energy from the acoustic mode and reduce its thermal occupation number. The effective occupation number $\bar{n}_{\text{eff}}$ is derived in Ref. [21], which is

$$\bar{n}_{\text{eff}} = \frac{\bar{n}}{1 - \mathcal{R}} + \bar{n}_{\text{quant}}. \quad (4)$$

Here the initial occupation number $\bar{n} \equiv [e^{\hbar\omega_m/(k_BT_0)} - 1]^{-1} \approx k_BT_0/(\hbar\omega_m)$, with $T_0$ denoting the environmental temperature. For large negative gain ($|\mathcal{R}| \gg 1$), the final achievable occupation number is set by the quantum limit $\bar{n}_{\text{quant}}$. In the tuned case $\Delta\omega = 0$, it is

$$\bar{n}_{\text{quant}} = \left(\frac{\gamma_1}{2\omega_m}\right)^2, \quad (5)$$

which is the same as the resolved-sideband limit derived in the pioneering work of Marquardt *et al.* [10] and Wilson-Rae *et al.* [11] for the conventional optoacoustic devices with one cavity transverse mode and one acoustic mode.

In addition, the strongly coupled OAPA naturally allows creation of stationary optoacoustic quantum entanglements. By simultaneously driving the two cavity transverse modes with large classical amplitude, we can achieve tripartite quantum entanglement among two cavity modes and the acoustic mode. The mathematical treatment is detailed in Ref. [21].

*Experimental feasibility.*—Even though the mathematical structure of three-mode OAPA is similar to its conventional two-mode counterpart, there are two significant differences from the experimental points of view. For the two-mode devices, the carrier light needs to be far detuned in order to achieve the resolved-sideband limit in the cooling experiment. The optoacoustic coupling strength is significantly limited by the available laser power, especially for a large-size acoustic resonator. The three-mode system naturally solves this issue by incorporating an additional cavity transverse mode. Both the carrier and the sideband fields are simultaneously resonant and coherently build up. This significantly enhances the optoacoustic coupling in the quantum regime, as also pointed out more recently by Dobrindt and Kippenberg [22]. In order to achieve the same optoacoustic coupling strength, the input optical power of the two-mode device needs to be $1 + (\Delta/\gamma)^2$ ($\Delta$ is cavity detuning, and $\gamma$ is the cavity linewidth) times larger than the three-mode one. It is a large factor $\sim$30 for the optimal cooling regime as suggested by Wilson-Rae *et al.* [11] and Genes *et al.* [12] with $\Delta \approx \omega_m$ and $\omega_m/\gamma \approx 5$.

Additionally, the laser phase and amplitude noise poses a problem in the conventional two-mode optoacoustic system for ground-state cooling. As first pointed out by Diósi [23] and later elaborated by Rabl *et al.* [24], the laser noise drives the acoustic resonator with a fluctuating force that sets a classical limit on the minimum achievable occupation number of the acoustic mode, while, for the three-mode OAPA, the laser noise is naturally evaded. A rigorous argument is the following: The optoacoustic interaction Hamiltonian for the two-mode system is given by $\hat{\mathcal{H}}_{\text{int}}^{\text{2-mode}} = \hbar G_0'\hat{q}_m\hat{a}^\dagger\hat{a}$, with coupling constant $G_0' \equiv \sqrt{\hbar\omega_0^2/(m\omega_m L^2)}$. The cavity mode $\hat{a}$ is driven externally with a large classical amplitude $\alpha(t)$. By replacing $\hat{a} \to \alpha(t) + \hat{a}$ and linearizing the Hamiltonian, we obtain

$$\hat{\mathcal{H}}_{\text{int}}^{\text{2-mode}} = \hbar G_0'\hat{q}_m[|\alpha(t)|^2 + \alpha^*(t)\hat{a} + \alpha(t)\hat{a}^\dagger]. \quad (6)$$

Because of the presence of term $|\alpha(t)|^2$, the fluctuations in the classical amplitude (i.e., amplitude and phase noises)

will impose a random force on the acoustic mode, thus increasing its effective occupation number. In contrast, for three-mode devices in the cooling regime, the $TEM_{00}$ mode is driven externally but the $TEM_{01}$ mode is not. After linearizing the interaction Hamiltonian in Eq. (1) with $\hat{a} \rightarrow \alpha(t) + \hat{a}$ and $\hat{b}$ unchanged, we have

$$\hat{\mathcal{H}}_{\text{int}}^{\text{3-mode}} = \hbar G_0 \hat{q}_m [\alpha^*(t)\hat{b} + \alpha(t)\hat{b}^\dagger]. \quad (7)$$

The classical fluctuating term $|\alpha(t)|^2$ vanishes at the leading order of interest. The three-mode device naturally achieves an equivalent interferometric configuration, which is insusceptible to the classical laser noise.

To confirm the physics of the three-mode OAPA, we used an 80 m suspended optical cavity with about 4 W of 1064 nm incident power and cylindrical sapphire mirrors of mass ~5.5 kg. We tuned the cavity transverse mode frequency using an electrically heated intracavity fused silica thermal tuning plate as shown schematically in Fig. 1(a). This plate acts as a variable focal length lens allowing the cavity $g$ factor to be tuned from 0.87 to 0.99, where the $g$ factor is defined as $g = (1 - L/R_1) \times (1 - L/R_2)$ for a cavity with length of $L$ and two end mirror radii of curvature of $R_1$ and $R_2$. When $g = 0.934$ and 0.981, the frequency differences between $TEM_{00}$ and $TEM_{01}$ modes are close to frequencies of acoustic modes at 160.0 and 84.8 kHz, respectively. As the transverse modes become resonant with the desired sideband frequency, Lorentzian peaks in the detected $TEM_{01}$ mode power are observed by a differential quadrant photodiode as shown in Fig. 1(b). We also confirmed linear transduction and correlation between the optical and acoustic signals by comparing the direct readout of acoustic modes excited in $M_2$ with the $TEM_{01}$ signal. In this experiment, we achieved a peak parametric gain at the level of $\sim 10^{-2}$ for both acoustic modes. Full details of these observations are presented in Ref. [20].

*Proposed experiment.*—As we can conclude from Eq. (2), the parametric gain is inversely proportional to the mass. Since the underlying principle applies to all scales, it would be much easier to achieve higher parametric gain with a low mass resonator. In Fig. 2, we propose a compact tabletop experimental setup of an OAPA. We incorporate an additional tuning cavity on top of the main interaction cavity which forms a pair of coupled cavities as suggested in Ref. [25]. The tuning cavity consists of mirrors $M_0$ and $M_1$ and a lens $L_1$ (or a concave mirror in a folded setup if optical loss was an issue). It can be viewed as an effective mirror but with mode- and frequency-dependent reflectivity, arising from the fact that the $TEM_{00}$ and $TEM_{01}$ modes experience different Guoy phase shift and propagating phase inside the tuning cavity. This setup allows us to continuously tune the frequency difference between the $TEM_{00}$ and $TEM_{01}$ modes such that both resonant positive and negative gain regimes are accessible by slightly changing the positions of $M_1$ and $L_1$. In this setup, the $TEM_{00}$ and $TEM_{01}$ modes can be independently detected from the transmitted light using an ordinary photodiode and a quadrant photodiode. The acoustic mode is also monitored by a capacitive readout. Independent readouts of optical and acoustic modes are crucial for revealing both the classical and quantum correlations among different modes.

The conditions for an OAPA to act as an acoustic mode amplifier or for creating self-sustained oscillation with $\mathcal{R} \sim 1$ are relatively easily accessible with current technology. As a numerical estimation, we choose the case of a milligram-scale mirror and $\omega_m/2\pi = 10^6$ Hz. In this case, $\mathcal{R} = 1$ is achieved with a cavity finesse of 5000, $Q_m = 10^5$, and 1 mW of a YAG laser incident power. In this case the OAPA acts as an acoustic amplifier, increasing the acoustic mode amplitude by the gain $1/(1 - \mathcal{R})$.

In order to achieve large parametric gain and eventually to realize quantum-ground-state cooling of the acoustic modes, low acoustic loss and a low environmental temperature are needed. Since optical coatings have high acoustic loss, it is essential that the coating mass contributes a small fraction of the resonator mass and that the part

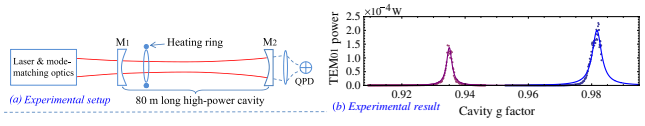


FIG. 1 (color online). Experimental demonstration of three-mode optoacoustic parametric interaction. (a) The schematic setup of the experiment. A thermal tuning plate was used to vary the cavity $g$ factor to tune the frequency difference between $TEM_{01}$ and $TEM_{00}$ modes. The resonant scattering of the $TEM_{01}$ mode is detected by a quadrant photodiode (QPD). (b) Experimental results fitted by a Lorentzian curve. The first peak corresponds to three-mode interactions with an acoustic mode at 160.0 kHz and the second one at 84.8 kHz. As the suspended cavity $g$ factor approaches unity, the cavity becomes extremely sensitive to angular fluctuations and unstable. Finally, it loses lock, and the data collection is ceased.

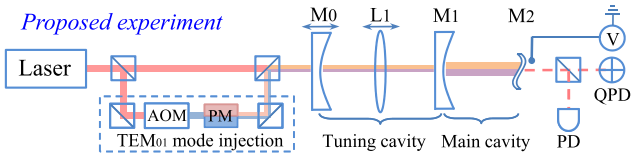


FIG. 2 (color online). Proposed experimental setup. A tuning cavity serves as an add-on to the main cavity to tune the frequency difference between $TEM_{00}$ and $TEM_{01}$ modes. An ordinary photodiode (PD), QPD, and a capacitive readout allow detections of the $TEM_{00}$, $TEM_{01}$, and acoustic modes independently. The $TEM_{01}$ mode injection is not required in the cooling experiment and only necessary for generating tripartite quantum entanglement. An acousto-optic modulator (AOM) and a phase mask (PM) create the right frequency and wave front for the $TEM_{01}$ mode.

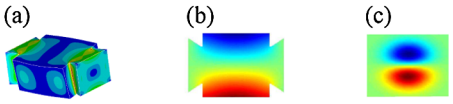


FIG. 3 (color online). Resonator design. (a) A silicon torsional mode resonator of dimensions $\sim 1$ mm $\times$ 0.8 mm $\times$ 0.5 mm and mass $\sim 1$ mg with resonant frequency $\sim 1$ MHz. The contours show the strain amplitude, which is concentrated in the spindle ends and minimum at the center where the $\mathrm{TEM}_{01}$ mode interacts. (b) Displacement distribution of the surface of the resonator torsional mode, showing a simple torsional displacement gradient along a central vertical axis. (c) The optical $\mathrm{TEM}_{01}$ mode amplitude distribution which has good overlap with the acoustic mode.

of the resonator supporting the mirror coatings be physically separated from the part experiencing large elastic deformation. The multilayer $\mathrm{Si\,O_2/Ta_2O_5}$ coatings required to achieve low optical loss have relatively large and roughly temperature-independent mechanical loss $\sim 10^{-4}$ [26]. Three-mode cooling makes it possible to cool much larger resonators (millimeter-scale) so that the coating mass fraction is small. Generally, the $Q$ factor is determined by [17] $Q^{-1} = Q_{\mathrm{int}}^{-1} + Q_{\mathrm{coating}}^{-1}(\Delta E/E)$, where $\Delta E$ is the strain energy stored in the coating and $E$ is the total strain energy of resonator mode concerned. We have modeled a milligram spindle shaped silicon torsional resonator which could be etched from a silicon wafer. It acts as a rigid body resonator and achieves a very good overlap to a $\mathrm{TEM}_{01}$ optical mode. The contours in Fig. 3(a) show the strain amplitude, which is concentrated in the spindle ends, and minimum at the center where the $\mathrm{TEM}_{01}$ mode interacts. The strain energy ratio $\Delta E/E$ is calculated to be $6.5 \times 10^{-4}$ with the coating area of 0.5 mm $\times$ 0.5 mm and thickness of 5 $\mu$m. Assuming $Q_{\mathrm{intrinsic}} \sim 10^8$ and $Q_{\mathrm{coating}} \sim 10^4$, the resulting $Q$ factor of the coated resonator will be $Q_m = 1.4 \times 10^7$. The resonator torsional mode displacement distribution and the $\mathrm{TEM}_{01}$ cavity mode amplitude distribution are shown in Fig. 3(b) and 3(c), respectively. This gives an overlap factor $\Lambda \sim 1$. For optical finesse of $5 \times 10^4$ and 50 mW input optical power (assuming an environmental temperature $\sim 4$ K), the final effective occupation number $\bar{n}_{\mathrm{eff}}$ of the acoustic mode for a 1 mg oscillator is approximately 0.1. As we have shown in Ref. [21], the same setup also allows us to explore stationary tripartite optoacoustic quantum entanglement. Because of the strong optoacoustic coupling through simultaneous buildup of both carrier and sideband fields, the entanglement is robust against environmental temperature and persists even when the environmental temperature goes up to 80 K.

*Conclusion.*—In conclusion, we have shown that by using three tuned resonant modes and a radiation pressure induced nonlinearity, strongly coupled optoacoustic parametric amplifiers can be created which are analogous to OPAs. We have shown that such interacting systems, first observed in an 80 m cavity, can be reduced to tunable centimeter-scale OAPA devices using three-mirror coupled cavities. We have shown that such OAPAs can be used to cool milligram-scale mechanical resonators to the quantum-ground state with practically achievable parameters. Besides opening a new method for exploration of fundamental quantum mechanics in macroscopic systems, the OAPA enables measurement at the single quanta level of displacement, mass, force, charge, or biological entities [27]. As strong sources of entanglement, they could find applications in quantum information, teleportation, and quantum encryption.

This research was supported by the Australian Research Council and the Department of Education, Science and Training. We thank Jesper Munch and Peter Veitch at The University of Adelaide and our collaborators Yanbei Chen, Phil Willems, David Reitze, Guido Muller, David Shoemaker, and Gregg Harry for invaluable discussions. We thank the LIGO Scientific Collaboration International Advisory Committee of the Gingin High Optical Power Facility for their support.

[1] M. Uenohara and J. Elward, Jr., IEEE Trans. Antennas Propag. **12**, 939 (1964).
[2] P. F. Cohadon *et al.*, Phys. Rev. Lett. **83**, 3174 (1999).
[3] C. Höberger and K. Karrai, Nature (London) **432**, 1002 (2004).
[4] S. Gigan *et al.*, Nature (London) **444**, 67 (2006).
[5] O. Arcizet *et al.*, Nature (London) **444**, 71 (2006).
[6] D. Kleckner and D. Bouwmeester, Nature (London) **444**, 75 (2006).
[7] A. Schliesser *et al.*, Phys. Rev. Lett. **97**, 243905 (2006); Nature Phys. **4**, 415 (2008).
[8] T. Corbitt *et al.*, Phys. Rev. Lett. **98**, 150802 (2007); **99**, 160801 (2007).
[9] J. D. Thompson *et al.*, Nature (London) **452**, 900 (2008).
[10] F. Marquardt *et al.*, Phys. Rev. Lett. **99**, 093902 (2007).
[11] I. Wilson-Rae *et al.*, Phys. Rev. Lett. **99**, 093901 (2007).
[12] C. Genes *et al.*, Phys. Rev. A **77**, 033804 (2008).
[13] D. Vitali *et al.*, Phys. Rev. Lett. **98**, 030405 (2007).
[14] M. Paternostro *et al.*, Phys. Rev. Lett. **99**, 250401 (2007).
[15] V. B. Braginsky *et al.*, Phys. Lett. A **287**, 331 (2001); **293**, 228 (2002); **305**, 111 (2002).
[16] C. Zhao *et al.*, Phys. Rev. Lett. **94**, 121102 (2005).
[17] L. Ju *et al.*, Phys. Lett. A **354**, 360 (2006).
[18] A. G. Gurkovsky *et al.*, Phys. Lett. A **362**, 91 (2007).
[19] S. Gras *et al.*, Phys. Lett. A **372**, 1348 (2008).
[20] C. Zhao *et al.*, Phys. Rev. A **78**, 023807 (2008).
[21] H. Miao *et al.*, Phys. Rev. A **79**, 063801 (2009).
[22] J. M. Dobrindt and T. J. Kippenberg, arXiv:0903.1013.
[23] L. Diósi, Phys. Rev. A **78**, 021801(R) (2008).
[24] P. Rabl *et al.*, arXiv:0903.1637.
[25] H. Maio *et al.*, Phys. Rev. A **78**, 063809 (2008).
[26] G. M. Harry *et al.*, Classical Quantum Gravity **19**, 897 (2002).
[27] T. J. Kippenberg *et al.*, Phys. Rev. Lett. **95**, 033901 (2005).